

Search for the sub-stellar lithium depletion boundary in the open star cluster Coma Berenices

E. L. Martín^{1,2,3}, N. Lodieu^{1,2}, and V. J. S. Béjar^{1,2}

¹ Instituto de Astrofísica de Canarias, Calle Vía Láctea s/n, E-38200 La Laguna, Tenerife, Spain

² Departamento de Astrofísica, Universidad de La Laguna, E-38206 La Laguna, Tenerife, Spain

³ Consejo Superior de Investigaciones Científicas, E-28006 Madrid, Spain

June 15, 2020

ABSTRACT

Aims. We mainly aim to search for the lithium depletion boundary (LDB) among the sub-stellar population of the open star cluster Coma Berenices.

Methods. Since the number of brown dwarf candidates in Coma Ber available in the literature is scarce, we carried out a search for additional candidates photometrically using colour-magnitude diagrams combining optical and infrared photometry from the latest public releases of the following large-scale surveys: the United Kingdom InfraRed Telescope Infrared Deep Sky Survey (UKIRT/UKIDSS), the Panoramic Survey Telescope and Rapid Response System (Pan-STARRS), the Sloan Digital Sky Survey (SDSS), and AllWISE. We checked astrometric consistency with cluster membership using *Gaia* DR2. A search for Li in three new and five previously known brown dwarf candidate cluster members was performed via spectroscopic observations using the OSIRIS instrument at the 10.4 m Gran Telescopio de Canarias (GTC).

Results. A couple dozen new photometric candidate brown dwarfs located inside the tidal radius of Coma Ber are reported, but none of these are significantly fainter and cooler than previously known members. No LiI resonance doublet at 6707.8 Å was detected in any of eight Coma Ber targets in the magnitude range J=15–19 and G=20–23 observed with the GTC. Spectral types and radial velocities were derived from the GTC spectra. These values confirm the cluster membership of four L2–L2.5 dwarfs, two of which are new in the literature.

Conclusions. The large Li depletion factors found among the four bona fide sub-stellar members in Coma Ber implies that the LDB must be located at spectral type later than L2.5 in this cluster. Using the latest evolutionary models for brown dwarfs, a lower limit of 550 Myr on the cluster age is set. This constraint has been combined with other dating methods to obtain an updated age estimate of 780±230 Myr for the Coma Ber open cluster. Identification of significantly cooler sub-stellar cluster members in Coma Ber awaits the advent of the Euclid wide survey, which should reach a depth of about J=23; this superb sensitivity will make it possible to determine the precise location of the sub-stellar LDB in this cluster and to carry out a complete census of its sub-stellar population.

Key words. Stars: low-mass — Stars: brown dwarfs — Galaxy: open clusters and association (Coma Berenices) — techniques: photometric — techniques: spectroscopic

1. Introduction

Characterization of brown dwarfs (BD) in open clusters is useful to test models of substellar evolution and to provide benchmarks to constrain ages and masses of BD candidates in the solar neighborhood. Particular interest has been devoted to the study of the most stable isotope of lithium (Li^7), which is destroyed in stellar interiors at temperatures above 2.5×10^6 K, i.e. before settling on the main-sequence, but not in BDs with masses below about $0.06 M_{\odot}$ (Magazzu et al. 1991; Pozio 1991; Rebolo et al. 1992), and hence detection of the Li I resonance doublet can be used to break degeneracies in the H-R diagram between stellar and sub-stellar mass objects (Magazzu et al. 1993; Martín et al. 1994a). In a coeval population, such as those of open clusters, the Li depletion boundary (LDB) provides a reliable dating method that has been used quite extensively in young open clusters and associations, such as for example the Pleiades (Stauffer et al. 1998) and IC 2602 (Dobbie et al. 2010).

Even though the range of applicability of the LDB method was thought to be restricted to ages between 20 and 200 Myr (Burke et al. 2004; Juárez et al. 2014), it has been shown recently that it can be extended to older clusters such as the Hyades, for

which an LDB age of 650 ± 70 Myr has been obtained (Lodieu et al. 2018b; Martín et al. 2018). The upper age limit to the application of the LDB in open clusters may take place at ages older than 1 Gyr when the Li brown dwarfs become so cold that atomic Li is no longer present in their atmospheres because it is locked in molecules such as LiH. So far, the coolest brown dwarfs for which a Li detection has been reported (Faherty et al. 2014; Lodieu et al. 2015) is the T0 secondary of the nearest brown dwarf binary (Luhman 2013).

Coma Berenices (hereafter abridged to Coma Ber, alternative name Melotte 111) is the second nearest open cluster to the Sun (86 pc; Tang et al. 2018; van Leeuwen 2009). Updated information about the cluster properties, including the identification of a leading and a trailing trail extending 50 pc away from the cluster center can be found in Tang et al. (2019). Coma Ber has a well defined core with a tidal radius of 6.9 pc, an elongated shape, tidal trails, and it is on its way to mixing with a nearby younger moving group and located 60 pc away from the cluster center (Fürnkranz et al. 2019; Tang et al. 2019). Coma Ber has solar metallicity and negligible reddening in the line of sight (Taylor

2006). The age has not been well determined, a wide range of ages are found in the literature (300–1000 Myr; Tsvetkov 1989).

Despite ongoing disruption, mass segregation, and the likely large loss of former members, Coma Ber still has about a hundred of low-mass stars (Kraus & Hillenbrand 2007), and it appears to have retained even some BDs still bound to the cluster. Candidate BD members in Coma Ber have been identified by Casewell et al. (2006). Follow-up spectra have been presented in Casewell et al. (2014) and their masses have been estimated to lie between 0.07 and 0.05 M_{\odot} , which straddle the range of masses where the LDB is expected to be located. Recently, Tang et al. (2018) used the parallaxes from the second data release of *Gaia* (Gaia Collaboration et al. 2018) to produce a full stellar census of Coma Ber and confirm one of the candidates in Casewell et al. (2014) as a bona-fide member. They identified two new substellar member candidates for which they assign tentative spectral types of L2 and L4 from low-resolution near-infrared spectra. These authors estimate a cluster age of 800 Myr from isochrone fitting of massive cluster members, an age significantly older than has been previously adopted in the literature (400–500 Myr; Kraus & Hillenbrand 2007).

In this paper, we present a photometric search for new faint objects in the core of Coma Ber, aimed at increasing the substellar population for LDB determination, and a spectroscopic search for Li among the coolest confirmed cluster members. In Section 2 we describe a photometric search of very low-mass (VLM) member candidates of Coma Ber cross-matching optical and near-infrared public surveys. In Section 3 we present low-resolution optical spectroscopy of eight very low-mass and potential BD member candidates collected with the optical spectrograph on the 10.4-m Gran Telescopio de Canarias (GTC). Four of them are confirmed as bona-fide substellar cluster members. In Section 4 we infer constraints on the age of Coma Ber from the absence of lithium in the four BD members confirmed by us and we provide a revised cluster age combining our results with other dating methods.

2. Search for very low-mass photometric candidate Coma Ber members

In order to increase the sample of BD targets for LDB determination in Coma Ber, our first step was to look for very red and faint photometric member candidates using the UKIRT Infrared Deep Sky Survey (UKIDSS; Lawrence et al. 2007) Galactic Clusters Survey (GCS) data release 9 (DR9). The search was limited to point sources fainter than 10 mag. to avoid saturation. Detections in both J and K bands with C Class parameters between -2 (probable point sources) and -1 (point sources) were required because L dwarfs have red J and K colors. We launched the query in the UKIRT Wide Field Camera (WFCAM; Casali et al. 2007) Science Archive (Hambly et al. 2008), which returned 234905 sources over an area of 98.8 square degrees. We show the GCS coverage in Coma Ber in Fig. 1 where we included the tidal radius of the cluster as a large cyan circle (6.9 pc; Tang et al. 2018). The GCS coverage does not reach out to the tidal tails of Coma Ber that extend up to 50 pc (Fürnkranz et al. 2019; Tang et al. 2018, 2019) but our survey is complete out to a radius of 5.6 deg centered at $(ra,dec) = (186.61,+26.31)$ degrees.

We cross-matched this input catalogue with the first data release of the Panoramic Survey Telescope and Rapid Response System (Pan-STARRS; Magnier et al. 2013), the Sloan Digital Sky Survey (SDSS Alam et al. 2015) DR12, and AllWISE (Cutri & et al. 2014; Wright et al. 2010) with a matching radius of 3

arcsec. We have included the calculation of the proper motions from the baseline between Pan-STARRS and SDSS data, whose mean value lies around 7.2 year. The similar numbers of sources in the UKIDSS GCS DR9 catalogue and the final catalogue with Pan-STARRS and SDSS show that both optical surveys perfectly complement the infrared photometry of the UKIDSS GCS. We show the GCS coverage in Coma Ber in Fig. 1.

To define conservative photometric selection cuts, we collected known members from the surveys of Casewell et al. (2006), Casewell et al. (2014), and Tang et al. (2018) and plotted in various colour-magnitude diagrams depicted in Fig. 2. The most recent survey of Tang et al. (2018) distinguishes candidates with and without parallaxes from the *Gaia* second data release (DR2) (Gaia Collaboration et al. 2018). We excluded three candidates of Casewell et al. (2006) that lie systematically below the sequence (candidate numbers #6, #11, and #13). The cluster sequence is mainly guided by the two faintest candidates of Tang et al. (2018) with infrared spectra: T159 and T191. The sequence of Hyades L dwarfs confirmed spectroscopically (Bouvier et al. 2008; Goldman et al. 2013; Hogan et al. 2008; Lodieu et al. 2018a; Martín et al. 2018) shifted to the distance of Coma Ber also supports the fact that the sequence of Coma Ber is marked by T159 and T191 (Tang et al. 2018), which we used as reference to define our selection lines. The object #12 (= cbd67) of Casewell et al. (2006) is confirmed as a L2.0 member and included in our selection. We note that the 500 Myr-old isochrone (Allard et al. 2012; Baraffe et al. 2015) and the field sequence of old M, L, and T dwarfs (Dupuy & Liu 2012) tend to lie above the putative sequence of very-low mass members in Coma Ber.

We defined photometric selection criteria in three colour-magnitudes diagrams with a set of straight lines going from the brightest to the faintest limits (green dashed lines in Fig. 2:

- $(J - K, J) \geq 0.73$ from $J = 11.2$ to 16 mag
- $(J - K, J) = (0.75, 16.0)$ to $(2.20, 20.0)$
- $(i_{PS1} - J, i_{PS1}) = (1.35, 12.2)$ to $(2.50, 18.2)$
- $(i_{PS1} - J, i_{PS1}) = (2.50, 18.2)$ to $(4.00, 22.5)$
- $(i_{PS1} - K, i_{PS1}) = (2.20, 12.2)$ to $(3.35, 18.2)$
- $(i_{PS1} - K, i_{PS1}) = (3.35, 18.2)$ to $(5.00, 22.5)$

We started off with the $(J - K, J)$ colour-magnitude because it is the most sensitive to red and faint cluster members. Then, we removed those not satisfying the criteria in the $(i - J, i)$ and $(i - K, i)$ diagrams, yielding a list of 2583 candidates labelled as “ComaBer: iK cand” in Fig. 2. We cross-matched this list with the *Gaia* DR2 catalogue to remove the 2550 sources with *Gaia* information because the astrometric selection was already done by Tang et al. (2018). We assume that this selection is complete down to the limit of *Gaia*, corresponding approximately to $J = 16$ mag. Hence, we are left with photometric candidates labelled as “ComaBer: NEW cand not in Gaia” and displayed as blue asterisks in Fig. 2. We should emphasise that our selection includes cbd10 and cbd67 as photometric candidates (Casewell et al. 2014) as well as T159 and T191 (Tang et al. 2018).

We computed the proper motions from the difference between the PS1 and SDSS positions, taking into account the epoch difference (mean or median around 7.25 years). The uncertainties on the proper motion is taken has 1.48 times the median absolute deviation (MAD). The MAD is 8.9 and 7.9 mas/yr, yielding proper motion uncertainties of 13.2 and 11.7 mas/yr in RA and dec, respectively. We analyse the position of these new photometric member candidates in the vector point diagram plotted in Fig. 3. We observe a large dispersion in the proper motions but find some sources with motions consistent with the bulk of parallax and photometric member candidates in Tang et al.

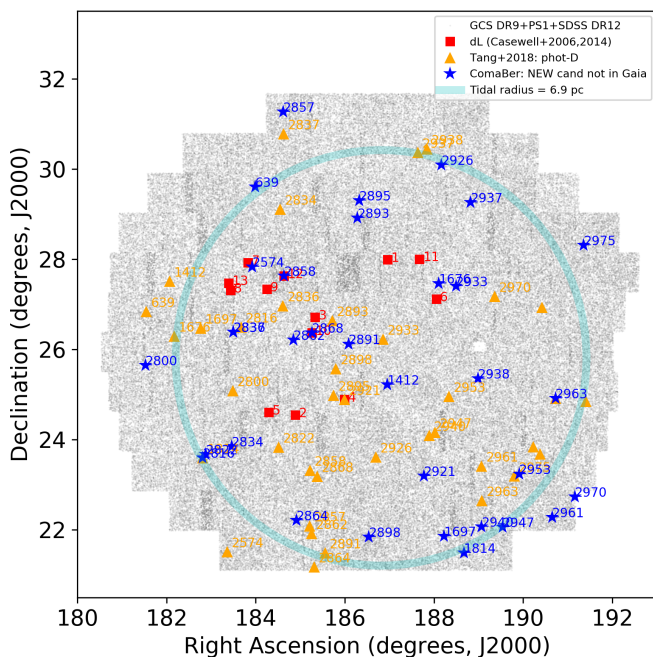


Fig. 1. Coverage of the full cross-matched catalogue with UKIDSS GCS, Pan-STARRS DR1, and SDSS DR12 photometric surveys (small grey dots). Overplotted with red squares, orange triangles, and blue asterisks are member candidates of the Coma Ber cluster from Casewell et al. (2006) and Casewell et al. (2014), Tang et al. (2018), and this study, respectively. We included the tidal radius of Coma Ber as a large cyan circle (6.9 pc; Tang et al. 2018).

(2018), e.g. #2963 = T191, #2816 = T159, #2938 = ComaBer4. If we apply a 3σ selection based on the uncertainties taken as $1.48 \times \text{MAD}$ and centered on the mean motion of the cluster ($-11.2, -9.2$ mas/yr), we would keep eight sources out of the 33 photometric candidates previously selected (#2963, 2893, 2816, 1412, 1697, 2938, 2940, 2970).

We compile this list of member candidates in Table 1, dividing it up into three sub-samples: (1) 4 sources previously reported by other studies (top panel), 8 photometric candidates with proper motion consistent with the mean motion of the cluster (middle panel), and the remaining 22 photometric candidates (bottom panel).

3. Spectroscopic observations and analysis

3.1. Low-resolution optical spectroscopy

We obtained optical spectra with the Optical System for Imaging and low Resolution Integrated Spectroscopy (OSIRIS; Cepa et al. 2000) instrument on the 10.4 m Gran Telescopio de Canarias (GTC) over two semesters (GTC47-18A and GTC55-19A; PI Martín). All of the data were collected under service mode, except four sources (ComaBer 4, 5, 7, and 13) which were observed during a 2-night visitor mode campaign on 12 and 13 May 2018 (observer V.J.S. Béjar). The log of the observations is available in Table 2. We requested dark conditions, seeing better than 1.2 arcsec, and spectroscopic conditions for both GTC programmes.

We obtained low-resolution optical spectra with the R1000R grating covering the 5100–10000 Å wavelength range and a slit of 1.2 arcsec, yielding a spectral resolving power of about 560 at the central wavelength. We acquired our targets in parallactic

angle with the Sloan z -band filter due to their faintness in the optical. We employed on-source integrations with the individual exposure times provided in Table 2, with 2 to 4 repeats shifted along the slit by 10 to 15 arcsec depending on the crowding of the field to allow for sky subtraction. As part of programme GTC55-19A, we also observed a nearby brown dwarf spectral standard with a clear lithium absorption, namely DENIS 1228 (Martín et al. 1997, 1999).

We reduced the data under the IRAF environment (Tody 1993) in a standard manner¹. First, we median-combined the bias and flat-fields taken during the afternoon, which we removed from the raw images. We extracted optimally each individual spectrum choosing the aperture and sky regions. We calibrated the spectra in wavelength with HgAr, Xenon, and Neon lamps with a rms better than 0.3 Å before averaging them to produce the final spectra shown in Fig. 4. We flux calibrated the 1D spectra with the response functions derived from two spectrophotometric standard stars: Hilt 600 (B1; Pancino et al. 2012) and Ross 640 (DZA5.5; Greenstein & Trimble 1967; Harrington & Dahn 1980; Wesemael et al. 1993) for programmes GTC47-18A and GTC55-19A, respectively. We did not correct for the second-order contamination so the flux calibration is solely valid up to 9500 Å.

3.2. Spectral typing

We normalised the OSIRIS spectra between 8240 Å and 8260 Å to compare with reference ultracool dwarfs of known spectral type because this wavelength range is located in a pseudocontinuum region in late-M dwarfs (Martín et al. 1996).

Spectral types were assigned to the targets by visual comparison with field late-M and early-L dwarfs from the SDSS database (Bochanski et al. 2007; Schmidt et al. 2010). A comparison of the spectra of one of our targets with the SDSS templates is shown in Fig. 5. The spectral types adopted in this work, and those from the literature for the sources in common, are listed in Table 3. We infer an optical spectral type of $M9.0 \pm 0.5$ for cbd34 (= T176) fully consistent with the infrared spectral types derived independently by Casewell et al. (2014) and Tang et al. (2018). This object is the warmest member candidate in our list of targets with GTC/OSIRIS optical spectra. We classify cbd10 as a $M9.5 \pm 0.5$ dwarf, which was lacking a spectrum in Casewell et al. (2014). We classify optically T159 as a $L2.0 \pm 0.5$ dwarf, again in agreement with the infrared spectral type in Table 4 of Tang et al. (2018). Its optical spectrum is similar to cbd67, previously classified as L1 in the near-infrared by Casewell et al. (2014), as well as to ComaBer 4, 5, and 7 to which we assign the same spectral type. The coolest object in our spectroscopic sub-sample is T191, classified optically as a $L2.5 \pm 0.5$, although we find it to be 1.5 sub-types earlier than the infrared classification of Tang et al. (2018, their Table 4).

3.3. Radial velocity measurements and cluster membership

RV measurements were obtained for all the targets from cross correlation with the spectrum of the template DENIS J1228 using the IRAF task *fxcor* over the spectral range 8100–10000 Å. Error bars were derived from gaussian fits to the correlation function. Heliocentric RV corrections were derived with the

¹ IRAF is distributed by the National Optical Astronomy Observatory, which is operated by the Association of Universities for Research in Astronomy (AURA) under cooperative agreement with the National Science Foundation

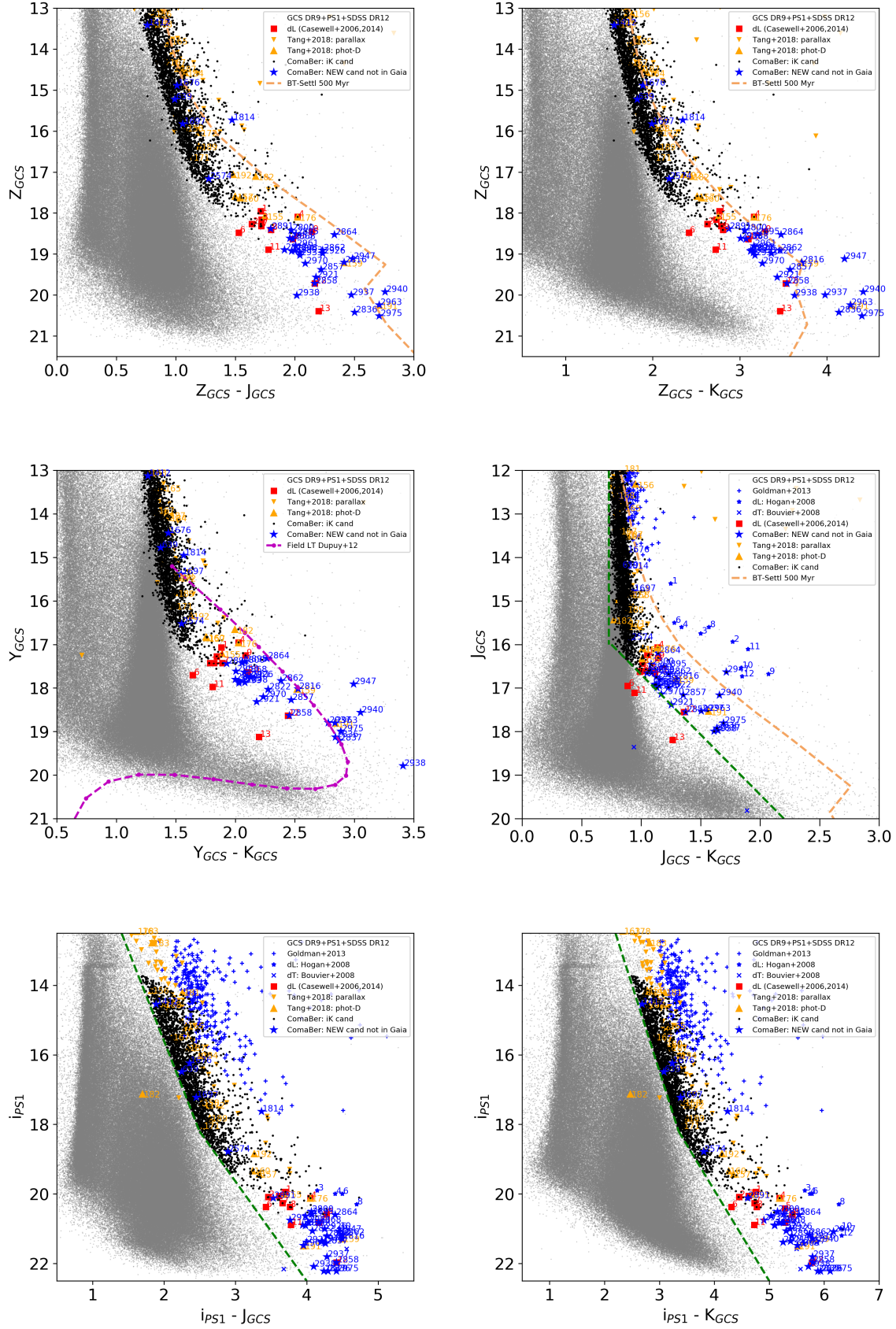


Fig. 2. Colour-magnitude diagrams with optical and infrared photometry from the GCS and Pan-STARRS surveys showing all sources common to UKIDSS GCS, Pan-STARRS DR1, and SDSS DR12 (small grey dots) along with iK candidates selected photometrically along the line of sight of Coma Ber. Overplotted are candidates from Casewell et al. (2006, 2014), Tang et al. (2018), and our study as red squares, orange triangles, and blue asterisks, respectively. We added the 500 Myr BT-Settl isochrones (Baraffe et al. 2015) as dashed orange lines and members in the Hyades (Bouvier et al. 2008; Goldman et al. 2013; Hogan et al. 2008), and the sequence of field ultracool dwarfs with known distances (magenta dashed line) for comparison in the diagrams where suitable photometric data are available. The selection cuts to identify photometric candidate members in Coma Ber are shown as green dashed lines.

Table 1. List of Coma Ber photometric member candidates identified in the area common to the three large-scale public surveys considered in this work. We list the ID number, the coordinates in sexagesimal format from UKIDSS GCS, and the infrared and optical photometry from UKIDSS GCS DR9, Pan-STARRS DR1, and SDSS DR12. *Top panel:* Four photometric candidates in common with earlier studies (Casewell et al. 2014; Tang et al. 2018). *Middle panel:* Eight photometric candidates with proper motion consistent with the mean motion of the cluster. *Bottom panel:* The remaining 22 photometric candidates. Notes: Known sources are: #2963 = T191, #2816 = T159, #2858 = cbd67, and #2868 = cbd10. Notes: New objects with GTC spectroscopy are: ComaBer 4 = #2938, ComaBer 5 = #2975, and ComaBer 7 = #2857.

ID	R.A.	Dec	Z	Y	J	H	K	PSi	PSz	PSy	SDSSu	SDSSg	SDSSr	SDSSi	SDSSz
	hh:mm:ss.s	°:':"	mag	mag	mag	mag	mag	mag	mag	mag	mag	mag	mag	mag	mag
2816	12:11:14.9	23:35:39.9	19.202	18.019	16.787	16.109	15.471	21.284	19.829	18.831	24.166	25.065	23.147	21.197	19.602
2858	12:18:32.7	27:37:30.8	19.719	18.632	17.551	16.779	16.183	21.970	20.508	19.476	26.364	25.419	23.700	22.328	20.154
2868	12:21:02.4	26:22:04.3	18.633	17.638	16.651	16.082	15.553	20.822	19.368	18.448	23.151	24.653	25.598	20.721	19.046
2963	12:42:53.7	24:55:07.1	20.240	18.807	17.530	16.688	15.924	21.485	20.674	19.719	23.854	24.751	24.571	22.577	20.381
1412	12:27:48.3	25:13:11.0	13.420	13.127	12.658	12.131	11.798	14.548	14.112	13.876	19.335	16.938	15.531	14.911	13.981
1697	12:32:54.2	21:51:17.1	15.830	15.384	14.771	14.183	13.855	17.224	16.480	16.108	22.789	20.356	18.807	17.208	16.306
2816	12:11:14.9	23:35:39.9	19.202	18.019	16.787	16.109	15.471	21.284	19.829	18.831	24.166	25.065	23.147	21.197	19.602
2893	12:25:06.9	28:54:48.0	18.966	17.839	16.923	16.361	15.860	20.907	19.533	18.629	25.068	25.042	24.801	20.936	19.313
2938	12:35:56.6	25:21:11.2	20.010	19.789	17.993	17.127	16.400	22.091	20.956	20.073	26.337	24.222	24.289	21.949	20.464
2940	12:36:15.9	22:03:45.7	19.924	18.560	17.165	16.292	15.564	21.370	20.483	19.347	24.868	25.350	25.395	22.100	20.033
2963	12:42:53.7	24:55:07.1	20.240	18.807	17.530	16.688	15.924	21.485	20.674	19.719	23.854	24.751	24.571	22.577	20.381
2970	12:44:37.8	22:43:41.9	19.228	18.205	17.139	16.494	15.971	21.357	20.005	18.993	24.756	24.382	23.646	21.333	19.463
639	12:15:57.2	29:36:20.8	15.228	14.778	14.237	13.714	13.391	16.486	15.818	15.505	22.654	19.573	18.007	16.500	15.703
1676	12:32:25.4	27:27:29.3	14.891	14.441	13.881	13.335	13.011	16.240	15.530	15.175	21.957	19.357	17.831	16.226	15.352
1814	12:34:40.5	21:29:25.8	15.732	14.953	14.258	13.797	13.397	17.627	16.390	15.770	24.560	21.886	20.452	17.634	16.197
2574	12:15:41.2	27:49:42.9	17.167	16.527	15.888	15.344	14.955	18.785	17.825	17.316	24.673	22.411	20.890	18.795	17.631
2800	12:06:06.0	25:38:35.5	18.420	17.422	16.449	15.857	15.359	20.516	19.109	18.236	24.163	24.698	23.804	20.648	18.871
2822	12:11:30.6	23:40:16.5	18.899	18.032	16.986	16.331	15.792	21.066	19.667	18.773	23.700	24.499	23.959	21.119	19.322
2834	12:13:50.1	23:50:42.7	18.926	17.801	16.953	16.314	15.803	20.897	19.488	18.564	24.951	25.181	24.520	20.624	19.147
2836	12:13:59.8	26:23:14.8	20.422	19.126	17.919	17.141	16.296	22.218	20.954	19.826	25.643	24.824	24.798	21.867	20.765
2857	12:18:27.2	31:15:53.3	19.382	18.276	17.162	16.357	15.767	21.427	20.085	19.241	23.334	23.950	23.602	21.355	19.808
2862	12:19:22.0	26:12:30.7	18.909	17.830	16.675	16.071	15.467	21.175	19.604	18.700	25.299	25.986	23.306	21.251	19.479
2864	12:19:38.4	22:12:36.2	18.531	17.321	16.198	15.570	15.013	20.599	19.142	18.155	25.500	25.154	22.837	20.410	18.561
2891	12:24:19.6	26:06:53.6	18.383	17.436	16.586	15.951	15.470	20.119	18.961	17.927	—	—	—	—	—
2895	12:25:16.4	29:18:04.2	18.518	17.396	16.506	15.847	15.276	20.578	19.210	18.322	23.374	22.171	21.348	19.873	18.152
2898	12:26:08.2	21:50:10.9	18.917	17.872	16.917	16.326	15.816	21.203	19.625	18.738	23.996	25.591	24.372	21.226	19.295
2921	12:31:04.5	23:11:42.6	19.566	18.315	17.388	16.648	16.130	21.386	19.949	19.099	25.349	24.812	23.786	21.537	19.840
2926	12:32:39.4	30:05:15.6	18.987	17.752	16.752	16.140	15.659	21.004	19.585	18.662	24.451	25.676	22.462	21.136	19.086
2933	12:33:58.2	27:24:12.6	19.032	17.887	16.989	16.335	15.816	20.759	19.520	18.667	23.533	24.009	23.446	21.041	19.158
2937	12:35:16.6	29:15:33.3	20.001	18.801	17.525	16.766	16.143	21.810	20.590	19.638	21.339	28.902	20.789	19.579	17.772
2947	12:38:09.0	22:03:32.2	19.116	17.909	16.631	15.684	14.895	21.086	19.738	18.839	25.316	25.322	23.387	21.183	19.364
2953	12:39:37.9	23:14:08.4	18.617	17.614	16.657	16.135	15.660	20.641	19.255	18.400	22.850	23.734	21.706	20.168	18.671
2961	12:42:35.8	22:16:43.9	18.806	17.746	16.797	16.134	15.688	20.822	19.446	18.524	25.025	24.623	23.428	20.966	19.123
2975	12:45:25.2	28:18:16.2	20.512	18.995	17.801	16.946	16.145	22.219	20.726	19.603	24.614	24.995	24.860	22.175	20.436

Table 2. Log of the GTC OSIRIS spectroscopic observations. We list the names of the targets as given in Casewell et al. (2006) and Tang et al. (2018), and this paper, respectively, along with their coordinates, magnitudes, dates of observations, instrumental set-up, weather conditions, and spectral types derived in this work. The last row is a well-known field lithium L dwarf template (Martín et al. 1997, 1999) observed as part of our programme GTC55-19A.

Name	R.A.	Dec	J	G	Date	Date	SNR
	hh:mm:ss.ss	°:':"	mag	mag	yyyy-mm-dd	sec	6750-6800 Å
cbd67	12:18:32.71	+27:37:31.3	17.551	22.485	13-04-2018	2×1800	4.9
cbd34	12:23:57.37	+24:53:29.0	15.940	20.140	13-04-2018	2×1500	12.9
cbd34	12:23:57.37	+24:53:29.0	15.940	20.140	13-05-2018	2×1500	7.8
cbd10	12:21:02.46	+26:22:04.2	16.814	21.139	12-04-2018	2×1500	2.0
ComaBer 4	12:35:56.59	+25:21:11.2	17.993	22.928	13-05-2018	2×1800	4.9
ComaBer 5	12:45:25.19	+28:18:16.2	17.801	22.736	13-05-2018	6×1800	7.0
ComaBer 7	12:18:27.25	+31:15:53.3	17.162	>21.36	12-05-2018	2×1500	3.6
T159	12:11:14.90	+23:35:39.9	16.787	22.736	29-04-2018	2×1800	3.9
T191	12:42:53.70	+24:55:07.1	17.530	22.736	29-04-2018	4×1960	4.1
T191	12:42:53.70	+24:55:07.1	17.530	22.736	01-05-2018	2×1960	3.2
T191	12:42:53.70	+24:55:07.1	17.530	22.736	11-05-2018	2×1960	7.6
DENIS1228	12:28:15.20	-15:47:34.2	14.378	—	13-04-2018	2×370	10.1

Table 3. Spectral types and radial velocities derived in this work. Spectral types from the literature come from Casewell et al. (2014) and Tang et al. (2018). Targets are ordered from earlier to later spectral subclass.

Name	SpT		RVs
	Literature	This work	km/s
cbd34	M9	M9.0±0.5	-2±38
cbd10		M9.5±0.5	3±46
cbd67	L1	L2.0±0.5	-18±35
ComaBer 4		L2.0±0.5	16±24
ComaBer 5		L2.0±0.5	2±15
ComaBer 7		L2.0±0.5	62±16
T159	L2	L2.0±0.5	10±21
T191	L4	L2.5±0.5	-1±14

Table 4. Pseudo EWs of atomic lines in targets observed with GTC/OSIRIS.

Name	H α	Li I	Rb I	Rb I	Na I	Cs I	Cs I
	6562.8 Å	6707.8 Å	7800.3 Å	7947.6 Å	8190 Å	8521.1 Å	8943.0 Å
cbd34	-2.6±0.8	<1.0	1.0±0.3	2.0±0.3	5.5±0.2	1.5±0.5	1.8±0.5
cbd10	>-2.3	<3.0	<1.0	2.2±0.5	4.9±0.5	<1.0	<0.5
cbd67	>-2.1	<1.1	2.3±0.6	1.9±0.7	5.8±0.9	3.2±0.6	2.9±0.4
ComaBer4	-5.5±0.8	<3.3	4.0±1.5	3.5±0.5	6.7±0.5	2.5±0.5	2.5±0.5
ComaBer5	-2.0±1.5	<1.5	2.4±0.2	1.5±0.5	5.1±0.2	3.1±0.3	1.7±0.2
ComaBer7	>-4.0	<3.0	5.0±0.5	3.4±0.2	6.1±0.3	2.9±0.5	1.3±0.3
T159	>-4.0	<2.0	3.1±0.3	2.3±0.5	5.5±0.3	1.8±0.5	1.9±0.2
T191	>-1.5	<1.2	4.9±0.4	4.6±0.9	4.7±0.3	2.3±0.7	3.0±0.4
DENIS1228	-1.75±0.25	2.6±0.6	4.7±1.5	6.5±0.5	4.9±0.3	4.6±0.3	4.3±0.2

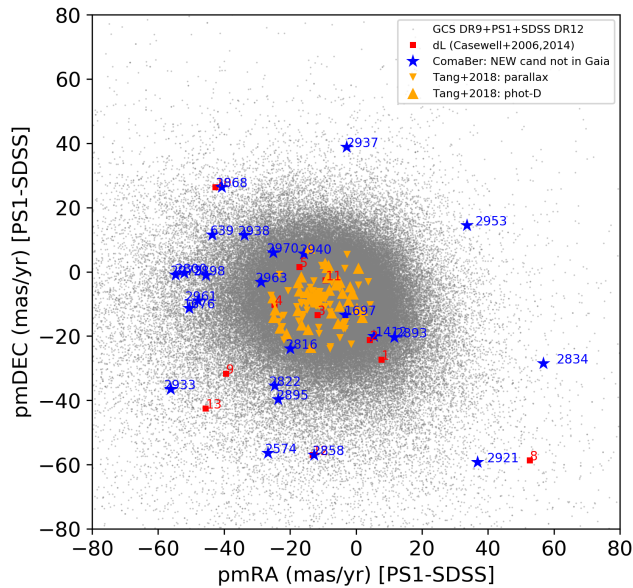


Fig. 3. Vector point diagram depicting the proper motions from the Pan-STARRS DR1, vs SDSS DR12 cross-match for all sources towards Coma Ber (grey dots). Overplotted are the photometric candidates selected in this work along with candidates from the literature (Casewell et al. 2014; Tang et al. 2018), as in Fig. 1.

IRAF task *rvcor*. Instrumental zeropoint correction was applied using a radial velocity of 4 km/s for DENIS J1228 (Martín et al. 1997). The measured radial velocities obtained for our targets

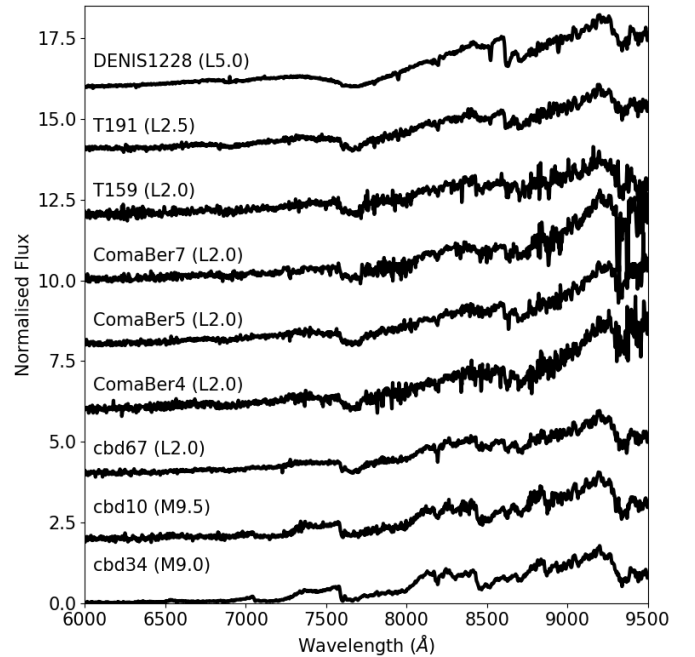


Fig. 4. Final set of GTC/OSIRIS spectra discussed in this paper. Spectral types assigned to each object are labelled.

and their uncertainties are provided in Table 3. The RV values of all but one of the Coma Ber targets are consistent within the error bars with the mean RV value of the cluster (-0.52 km/s) provided by *Gaia* DR2 (Gaia Collaboration et al. 2018). The exception is ComaBer7, which has a larger RV value of 62±16

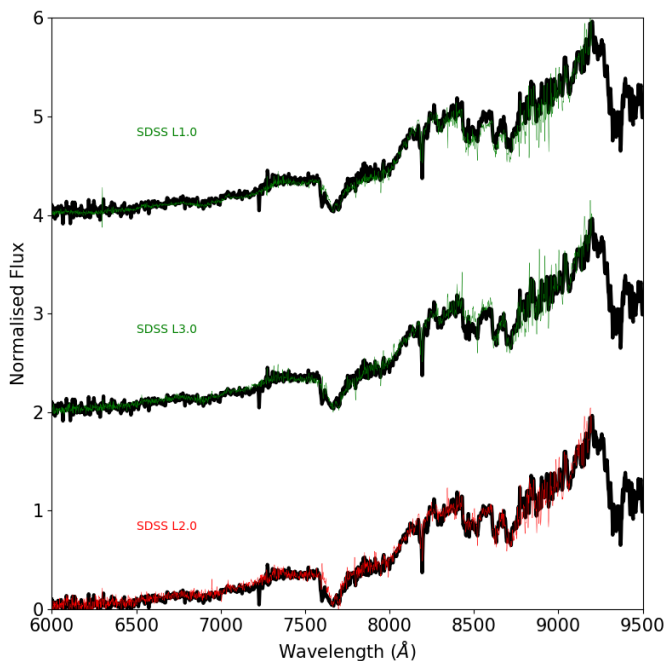


Fig. 5. GTC/OSIRIS optical spectra the BD candidate cbd67 (black thick line) compared with L dwarf templates from SDSS (green and red lines).

km/s, which deviates from the cluster RV by more than 3 times the uncertainty.

Since cbd67 has been deemed not to be a bona-fide member in Coma Ber because it does not have consistent proper motion (Tang et al. 2018), and ComaBer7 has a larger RV value than expected for a member in the cluster, we do not include these objects in the subset of confirmed cluster members. Therefore, only cbd10/34, ComaBer4/5, and T159/191 are retained as bona fide cluster members confirmed by our RV analysis. As a cautionary note, we remind the reader that ComaBer5 does not have membership confirmation by proper motion.

3.4. Pseudo equivalent width measurements

We searched for the presence of Li I in absorption at 6707.8\AA in the GTC/OSIRIS spectra. A zoom on the Li I spectral region is shown in Fig. 6 for a representative subset of our sample. The Li I resonance doublet clearly stands out from the noise only in our reference lithium L dwarf, DENIS1228 (Martín et al. 1997, 1999), but not in the Coma Ber targets. We did not detect the Li I feature in any of the Coma Ber spectra. Signal to Noise ratios (SNR) in a spectral region adjacent to the Li I spectral region were measured with the spot task in IRAF, and are given in Table 2. This region is the same as that used in Martín et al. (2018). The SNR values measured by us in the Coma Ber targets tend to be slightly lower than to those reported by Martín et al. (2018) for Hyades targets, and hence our uncertainties in pEW measurements are larger.

From these data we can only impose upper limits on the Li I pseudo-equivalent width (pEW) of the Coma Ber targets. Those upper limits, together with pEW measurements or upper limits on the emission of H_α , and other atomic lines of interest (Cs I, Na I and Rb I) are provided in Table 4. The pEW values were estimated independently by each author using the task spot in the IRAF environment. The mean value of each measurement was

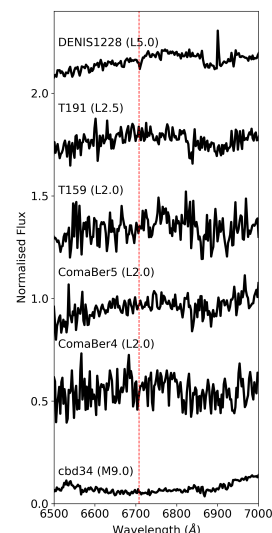


Fig. 6. Zoom on the spectral region around the Li resonance doublet at 6707.8\AA for Coma Ber objects found by us, and by Casewell et al. (2006), Casewell et al. (2014), and Tang et al. (2018), and confirmed as bona-fide cluster members in this work. The location of the Li I resonance doublet is marked with a vertical red line. This feature is clearly detected only in the GTC/OSIRIS spectrum of the lithium L dwarf, DENIS1228 (Martín 1997; Martín et al. 1999), but not in the Coma Ber targets.

adopted and the error bar reflects the dispersion in the values obtained. The pEW values of the Cs I and Li I features obtained from our spectrum of DENIS1228 are consistent within the measurement uncertainties with those reported by Kirkpatrick et al. (1999) and Martín et al. (1999). On the other hand, for the Na I doublet our value is significantly stronger than the one given by Martín et al. (1999). This could be due to the fact that we partially resolve the Na I doublet, whereas it is completely blended in the KeckII data presented in Martín et al. (1999), and to contamination by telluric absorption in the red part of the feature.

Weak H_α in emission is detected in 3 out of the 6 Coma Ber members. The frequency of H_α emitters among Coma Ber M9–L2.5 objects (50%) is higher than among high-gravity field dwarfs in the same range of spectral subclasses (8 out of 34; 23.5%) (Martín et al. 2010) suggesting that chromospheric activity is stronger in the Coma Ber substellar population because it is younger than the field.

Low-gravity field dwarfs with spectral subclasses from M9 to L0 are thought to have ages younger than about 100 Myr. They have Na I pEW values below 4\AA , and H_α pEW values stronger than $\text{pEW} = -14\text{\AA}$ (Martín et al. 2010). None of the targets observed by us have as weak Na I and as strong H_α emission as low-gravity field dwarfs, indicating that they are older, high-gravity ultracool dwarfs.

4. Lithium depletion and the age of Coma Ber

The upper limits to the pEW of the Li I resonance doublet reported in Table 4, were converted to Li abundances using the method described in Martín et al. (2018), and the same initial Li abundance of $\log N(\text{Li})=3.3$ as in the Hyades, which is thought to be representative of the cosmic Li content in newly born stars (Martín 1997; Martín et al. 1994b).

Since Coma Ber is not much younger than the Hyades, it is likely that the L-type members are BDs, but this is not guaran-

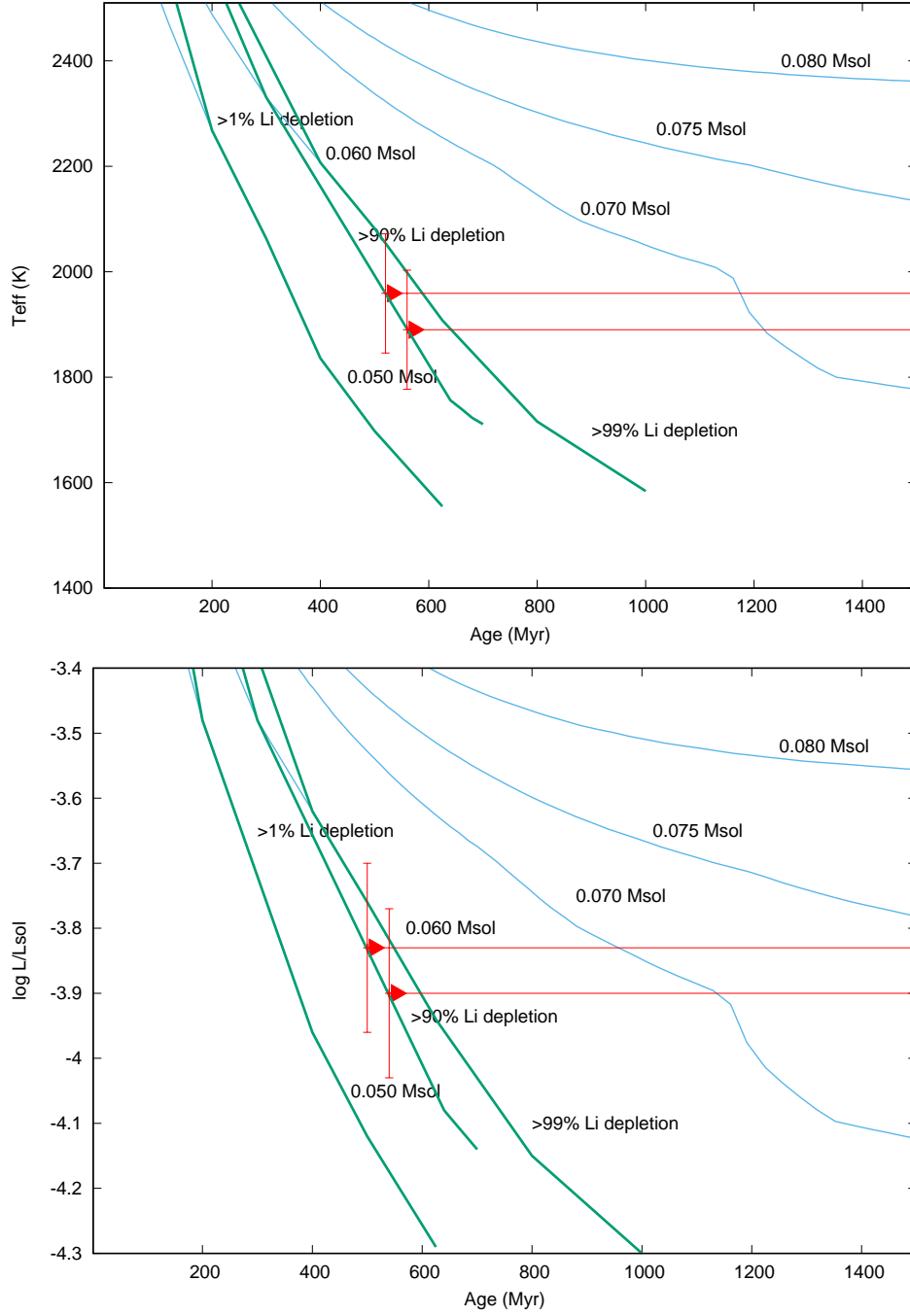


Fig. 7. Evolutionary tracks (effective temperature (T_{eff}) and luminosity) from the models by Baraffe et al. (2015) for VLM stars and BDs as a function of age. Masses and predicted Li depletion factors are labeled. The non detection of Li in the Coma Ber member candidates studied in this work impose lower limits on the cluster age. The limit coming from the L2 candidates is depicted as the upper red triangle and horizontal line, and the limit obtained from the L2.5 object (T191) corresponds to the lower triangle and horizontal line in red colour.

Table 5. Basic parameters and Li abundances for RV confirmed substellar members in Coma Ber.

Name	SpT	$\log(L_{bol}/L_{\odot})$	T_{eff} (K)	$\log N(\text{Li})$	Age (Myr)
ComaBer 4	L2.0 \pm 0.5	-3.83 \pm 0.13	1959 \pm 113	<2.4	>480
ComaBer 5	L2.0 \pm 0.5	-3.83 \pm 0.13	1959 \pm 113	<1.8	>500
T159	L2.0 \pm 0.5	-3.83 \pm 0.13	1959 \pm 113	<2.0	>490
T191	L2.5 \pm 0.5	-3.90 \pm 0.13	1890 \pm 113	<1.5	>550

Table 6. Li depletion boundary (LDB) in open clusters older than 20 Myr, ordered by increasing distance.

Name	d	SpT	Age (LDB)	Age (Other)	Mass	Ref.
	pc	Li	Myr	Myr	Msun	
Hyades	47	L4	650±70	570 – 900	0.065	Martín et al. (2018)
Coma Ber	87	>L2.5	>550	300 – 1000	<0.07	This work
Pleiades	130	M6.5	112±5	70 – 160	0.075	Dahm (2015)
IC 2391	146	M5	50±5	30 – 75	0.12	Barrado y Navascués et al. (2004)
IC 2602	152	M5.5	46±6	25 – 70	0.12	Dobbie et al. (2010)
Alpha Per	190	M6.5	85±10	50–70	0.08	Barrado y Navascués et al. (2004)
Blanco 1	207	M7	126±14	150 – 500	0.072	Juarez et al. (2014)
IC 4665	385	M4	28±5	30 – 100	0.24	Manzi et al. (2008)
NGC 2547	430	M4	35±4	20–80	0.17	Jeffries & Oliveira (2005)

teed for the late-M members. In the following discussion, we retain only the bona-fide substellar cluster members, i.e., the L-type brown dwarfs confirmed by us with radial velocities. As discussed by Martín et al. (2018), it is well justified to use the calibrations for field L dwarfs of known distance to calculate the bolometric luminosities ($\log(L_{\text{bol}}/L_{\odot})$) and effective temperatures (T_{eff}) from the spectral types obtained by us for the cluster members. The values obtained using the calibrations from Filipazzo et al. (2015) are provided in Table 5.

The lack of Li detection implies that the Coma Ber BDs have depleted significant amounts of this light element, which in turn can be used to derive constraints on the age of the cluster using evolutionary models. In our previous work in the Hyades (Martín et al. 2018), we found that there is good agreement between the Li depletion age constraints and other parameters such as luminosity and temperature for the models by (Baraffe et al. 2015), and thus we adopt the same models in this work, as illustrated in Fig. 7. From these models, and the Li depletion factors obtained among the substellar members in Coma Ber, we infer a lower limit on the cluster age of 550 Myr. The limit obtained from the L2.5 member (T191) is 50 Myr more stringent than from the L2.0 members. Age estimates for Coma Ber have ranged from 300 Myr to 1000 Myr (Tsvetkov 1989). For example, Kraus & Hillenbrand (2007) used an age of 400 Myr in their study of the low-mass population. The lower limit on the age derived in this work restricts the allowed range of ages for Coma Ber to lie between 550 Myr and 1000 Myr, and hence we propose a revised age estimate of 780 ± 230 Myr, which is consistent with the age estimates in the range 700 – 800 Myr proposed by Tang et al. (2018, 2019) from analysis of a few post-main sequence stars.

A more precise age estimate for this cluster could be derived from Li detection in members cooler than those studied here. We plan to carry out a search for fainter Coma Ber members using the Euclid wide survey in the framework of the project Independent Legacy Science on ultracool dwarfs, which was selected by ESA in 2012. According to the Euclid specifications, the wide survey should reach about 5 mag. deeper in optical and near-infrared passbands than the surveys that we have used in this work. If the age of Coma Ber is as old or older than that of the Hyades, the LDB should be located at spectral type later than L3. Li has been detected in L3.5–L5 members in the Hyades (Lodieu et al. 2018a; Martín et al. 2018). Similar observations in L dwarfs in Coma Ber would be challenging but not unfeasible, and they are critical to refine the age of Coma Ber using the substellar Li boundary method.

Coma Ber is the second open cluster closest to us, and also the second one known for which the LDB age is older than 500

Myr. In Table 6 we put our LDB results for Coma Ber in context with previous results for other open clusters older than 20 Myr. Note that the results reported here, together with those in the Hyades, have significantly extended the range of applicability of the LDB method.

As can be seen in Table 6, where the spectral type of the objects where Li reemerges in different open clusters is listed in column 3, the LDB evolves from mid-M spectral types at very young ages (20–50 Myr) to mid-L dwarfs at more mature ages (600–700 Myr). Since BDs keep cooling down with increasing time, the LDB method can still be applied to even older open clusters, moving groups, associations or multiple stellar systems, although it will be harder because the substellar-mass members are much fainter than in younger open clusters, and Li may be locked up in molecules in T dwarfs. In Coma Ber we are already reaching the practical limit of what can be done with a 10-m class telescope in a reasonable amount of observing time. The new generation of larger optical telescopes will be needed to extend this work to more distant and/or older clusters such as, for example, Praesepe, where BD candidates have already been identified (Magazzù et al. 1998; Wang et al. 2011), and which has an age similar to Coma Ber although it is located more than twice further away (Lodieu et al. 2019).

The LDB method is orthogonal to other dating methods such as isochrone fitting and gyrochronology, and tends to provide rather precise values that could be useful to constrain the wider range of estimates obtained from different stellar clocks. The validity of the LDB now extends for over a factor of 3 in mass and over a factor of 30 in age, and it provides a promising method to calibrate traditional models of evolved intermediate-mass stars, low-mass pre-main sequence stars, and young main sequence stars.

Acknowledgements. Based on observations made with the Gran Telescopio Canarias (GTC), installed in the Spanish Observatorio del Roque de los Muchachos of the Instituto de Astrofísica de Canarias, in the island of La Palma (programmes GTC47-18A and GTC55-19A). ELM, NL, and VJSB were financially supported by the Ministerio de Economía y Competitividad and the Fondo Europeo de Desarrollo Regional (FEDER) under grants AYA2015-69350-C3-1-P and AYA2015-69350-C3-2-P. This research has made use of the Simbad and Vizieur databases, operated at the centre de Données Astronomiques de Strasbourg (CDS), and of NASA’s Astrophysics Data System Bibliographic Services (ADS). This research has also made use of some of the tools developed as part of the Virtual Observatory. This work has made use of data from the European Space Agency (ESA) mission *Gaia* (<https://www.cosmos.esa.int/gaia>), processed by the *Gaia* Data Processing and Analysis Consortium (DPAC, <https://www.cosmos.esa.int/web/gaia/dpac/consortium>). Funding for the DPAC has been provided by national institutions, in particular the institutions participating in the *Gaia* Multilateral Agreement. Funding for the Sloan Digital Sky Survey IV has been provided by the Alfred P. Sloan Foundation, the U.S. Department of Energy Office of Science, and the Participating Institutions. SDSS-IV acknowledges support and resources from

the Center for High-Performance Computing at the University of Utah. The SDSS web site is www.sdss.org. SDSS-IV is managed by the Astrophysical Research Consortium for the Participating Institutions of the SDSS Collaboration including the Brazilian Participation Group, the Carnegie Institution for Science, Carnegie Mellon University, the Chilean Participation Group, the French Participation Group, Harvard-Smithsonian Center for Astrophysics, Instituto de Astrofísica de Canarias, The Johns Hopkins University, Kavli Institute for the Physics and Mathematics of the Universe (IPMU) / University of Tokyo, Lawrence Berkeley National Laboratory, Leibniz Institut für Astrophysik Potsdam (AIP), Max-Planck-Institut für Astronomie (MPIA Heidelberg), Max-Planck-Institut für Astrophysik (MPA Garching), Max-Planck-Institut für Extraterrestrische Physik (MPE), National Astronomical Observatories of China, New Mexico State University, New York University, University of Notre Dame, Observatório Nacional / MCTI, The Ohio State University, Pennsylvania State University, Shanghai Astronomical Observatory, United Kingdom Participation Group, Universidad Nacional Autónoma de México, University of Arizona, University of Colorado Boulder, University of Oxford, University of Portsmouth, University of Utah, University of Virginia, University of Washington, University of Wisconsin, Vanderbilt University, and Yale University. This publication makes use of data products from the Two Micron All Sky Survey, which is a joint project of the University of Massachusetts and the Infrared Processing and Analysis Center/California Institute of Technology, funded by the National Aeronautics and Space Administration and the National Science Foundation.

The UKIDSS project is defined in Lawrence et al. (2007). UKIDSS uses the UKIRT Wide Field Camera Casali et al. (WFCAM; 2007). The photometric system is described in Hewett et al. (2006), and the calibration is described in Hodgkin et al. (2009). The pipeline processing and science archive are described in Irwin et al. (2009, in prep) and Hambly et al. (2008).

This publication makes use of data products from the Wide-field Infrared Survey Explorer, which is a joint project of the University of California, Los Angeles, and the Jet Propulsion Laboratory/California Institute of Technology, and NEOWISE, which is a project of the Jet Propulsion Laboratory/California Institute of Technology. WISE and NEOWISE are funded by the National Aeronautics and Space Administration.

The Pan-STARRS1 Surveys (PS1) and the PS1 public science archive have been made possible through contributions by the Institute for Astronomy, the University of Hawaii, the Pan-STARRS Project Office, the Max-Planck Society and its participating institutes, the Max Planck Institute for Astronomy, Heidelberg and the Max Planck Institute for Extraterrestrial Physics, Garching, The Johns Hopkins University, Durham University, the University of Edinburgh, the Queen's University Belfast, the Harvard-Smithsonian Center for Astrophysics, the Las Cumbres Observatory Global Telescope Network Incorporated, the National Central University of Taiwan, the Space Telescope Science Institute, the National Aeronautics and Space Administration under Grant No. NNX08AR22G issued through the Planetary Science Division of the NASA Science Mission Directorate, the National Science Foundation Grant No. AST-1238877, the University of Maryland, Eotvos Lorand University (ELTE), the Los Alamos National Laboratory, and the Gordon and Betty Moore Foundation.

Gaia Collaboration, Brown, A. G. A., Vallenari, A., et al. 2018, *A&A*, 616, A1
 Goldman, B., Röser, S., Schilbach, E., et al. 2013, *A&A*, 559, A43
 Greenstein, J. L. & Trimble, V. L. 1967, *ApJ*, 149, 283
 Hambly, N. C., Collins, R. S., Cross, N. J. G., et al. 2008, *MNRAS*, 384, 637
 Harrington, R. S. & Dahn, C. C. 1980, *AJ*, 85, 454
 Hewett, P. C., Warren, S. J., Leggett, S. K., & Hodgkin, S. T. 2006, *MNRAS*, 367, 454
 Hodgkin, S. T., Irwin, M. J., Hewett, P. C., & Warren, S. J. 2009, *MNRAS*, 394, 675
 Hogan, E., Jameson, R. F., Casewell, S. L., Osbourne, S. L., & Hambly, N. C. 2008, *MNRAS*, 388, 495
 Jeffries, R. D. & Oliveira, J. M. 2005, *MNRAS*, 358, 13
 Juárez, A. J., Cargile, P. A., James, D. J., & Stassun, K. G. 2014, *ApJ*, 795, 143
 Kirkpatrick, J. D., Reid, I. N., Liebert, J., et al. 1999, *ApJ*, 519, 802
 Kraus, A. L. & Hillenbrand, L. A. 2007, *AJ*, 134, 2340
 Lawrence, A., Warren, S. J., Almaini, O., et al. 2007, *MNRAS*, 379, 1599
 Lodieu, N., Pérez-Garrido, A., Smart, R. L., & Silvotti, R. 2019, *A&A*, 628, A66
 Lodieu, N., Rebolo, R., & Pérez-Garrido, A. 2018a, *A&A*, 615, L12
 Lodieu, N., Zapatero Osorio, M. R., Béjar, V. J. S., & Peña Ramírez, K. 2018b, *MNRAS*, 473, 2020
 Lodieu, N., Zapatero Osorio, M. R., Rebolo, R., et al. 2015, *A&A*, 581, A73
 Luhman, K. L. 2013, *ApJL*, 767, L1
 Magazzu, A., Martin, E. L., & Rebolo, R. 1991, *A&A*, 249, 149
 Magazzu, A., Martin, E. L., & Rebolo, R. 1993, *ApJL*, 404, L17
 Magazzù, A., Rebolo, R., Zapatero Osorio, M. R., Martín, E. L., & Hodgkin, S. T. 1998, *ApJ*, 497, L47
 Magnier, E. A., Schlafly, E., Finkbeiner, D., et al. 2013, *ApJS*, 205, 20
 Manzi, S., Randich, S., de Wit, W. J., & Palla, F. 2008, *A&A*, 479, 141
 Martín, E. L. 1997, *A&A*, 321, 492
 Martín, E. L., Basri, G., Delfosse, X., & Forveille, T. 1997, *A&A*, 327, L29
 Martín, E. L., Delfosse, X., Basri, G., et al. 1999, *AJ*, 118, 2466
 Martín, E. L., Lodieu, N., Pavlenko, Y., & Béjar, V. J. S. 2018, *ApJ*, 856, 40
 Martín, E. L., Phan-Bao, N., Bessell, M., et al. 2010, *A&A*, 517, A53
 Martín, E. L., Rebolo, R., & Magazzu, A. 1994a, *ApJ*, 436, 262
 Martín, E. L., Rebolo, R., Magazzu, A., & Pavlenko, Y. V. 1994b, *A&A*, 282, 503
 Martín, E. L., Rebolo, R., & Zapatero Osorio, M. R. 1996, *ApJ*, 469, 706
 Pancino, E., Altavilla, G., Marini, S., et al. 2012, *MNRAS*, 426, 1767
 Pozio, F. 1991, *Mem. Soc. Astron. Italiana*, 62, 171
 Rebolo, R., Martín, E. L., & Magazzù, A. 1992, *ApJL*, 389, L83
 Schmidt, S. J., West, A. A., Hawley, S. L., & Pineda, J. S. 2010, *AJ*, 139, 1808
 Stauffer, J. R., Schultz, G., & Kirkpatrick, J. D. 1998, *ApJL*, 499, 199
 Tang, S.-Y., Chen, W. P., Chiang, P. S., et al. 2018, *ApJ*, 862, 106
 Tang, S.-Y., Pang, X., Yuan, Z., et al. 2019, *ApJ*, 877, 12
 Taylor, B. J. 2006, *AJ*, 132, 2453
 Tody, D. 1993, in *Astronomical Society of the Pacific Conference Series*, Vol. 52, *Astronomical Data Analysis Software and Systems II*, ed. R. J. Hanisch, R. J. V. Brissenden, & J. Barnes, 173
 Tsvetkov, T. G. 1989, *Astrophys. Space. Sci.*, 151, 47
 van Leeuwen, F. 2009, *A&A*, 497, 209
 Wang, W., Boudreault, S., Goldman, B., et al. 2011, *A&A*, 531, A164
 Wesemael, F., Greenstein, J. L., Liebert, J., et al. 1993, *PASP*, 105, 761
 Wright, E. L., Eisenhardt, P. R. M., Mainzer, A. K., et al. 2010, *AJ*, 140, 1868

References

Alam, S., Albareti, F. D., Allende Prieto, C., et al. 2015, *ApJS*, 219, 12
 Allard, F., Homeier, D., & Freytag, B. 2012, *Royal Society of London Philosophical Transactions Series A*, 370, 2765
 Baraffe, I., Homeier, D., Allard, F., & Chabrier, G. 2015, *A&A*, 577, A42
 Barrado y Navascués, D., Stauffer, J. R., & Jayawardhana, R. 2004, *ApJ*, 614, 386
 Bochanski, J. J., West, A. A., Hawley, S. L., & Covey, K. R. 2007, *AJ*, 133, 531
 Bouvier, J., Kendall, T., Meeus, G., et al. 2008, *A&A*, 481, 661
 Burke, C. J., Pinsonneault, M. H., & Sills, A. 2004, *ApJ*, 604, 272
 Casali, M., Adamson, A., Alves de Oliveira, C., et al. 2007, *A&A*, 467, 777
 Casewell, S. L., Jameson, R. F., & Dobbie, P. D. 2006, *MNRAS*, 365, 447
 Casewell, S. L., Littlefair, S. P., Burleigh, M. R., & Roy, M. 2014, *ArXiv e-prints*
 Cepa, J., Aguiar, M., Escalera, V. G., et al. 2000, in *Society of Photo-Optical Instrumentation Engineers (SPIE) Conference Series*, Vol. 4008, *Society of Photo-Optical Instrumentation Engineers (SPIE) Conference Series*, ed. M. Iye & A. F. Moorwood, 623–631
 Cutri, R. M. & et al. 2014, *VizieR Online Data Catalog*, 2328, 0
 Dahm, S. E. 2015, *ApJ*, 813, 108
 Dobbie, P. D., Lodieu, N., & Sharp, R. G. 2010, *MNRAS*, 409, 1002
 Dupuy, T. J. & Liu, M. C. 2012, *ApJS*, 201, 19
 Faherty, J. K., Beletsky, Y., Burgasser, A. J., et al. 2014, *ApJ*, 790, 40
 Filippazzo, J. C., Rice, E. L., Faherty, J., et al. 2015, *ApJ*, 810, 158
 Fürnkranz, V., Meingast, S., & Alves, J. 2019, *A&A*, 624, L11